Supporting Information to:

Accurate determination of the orientational distribution of a fluorescent dye in a phospholipid membrane: Interplay between linear dichroism measurements and molecular simulations

1. Atom Types, Atomic Charges, and Charge Groups of F2N12S

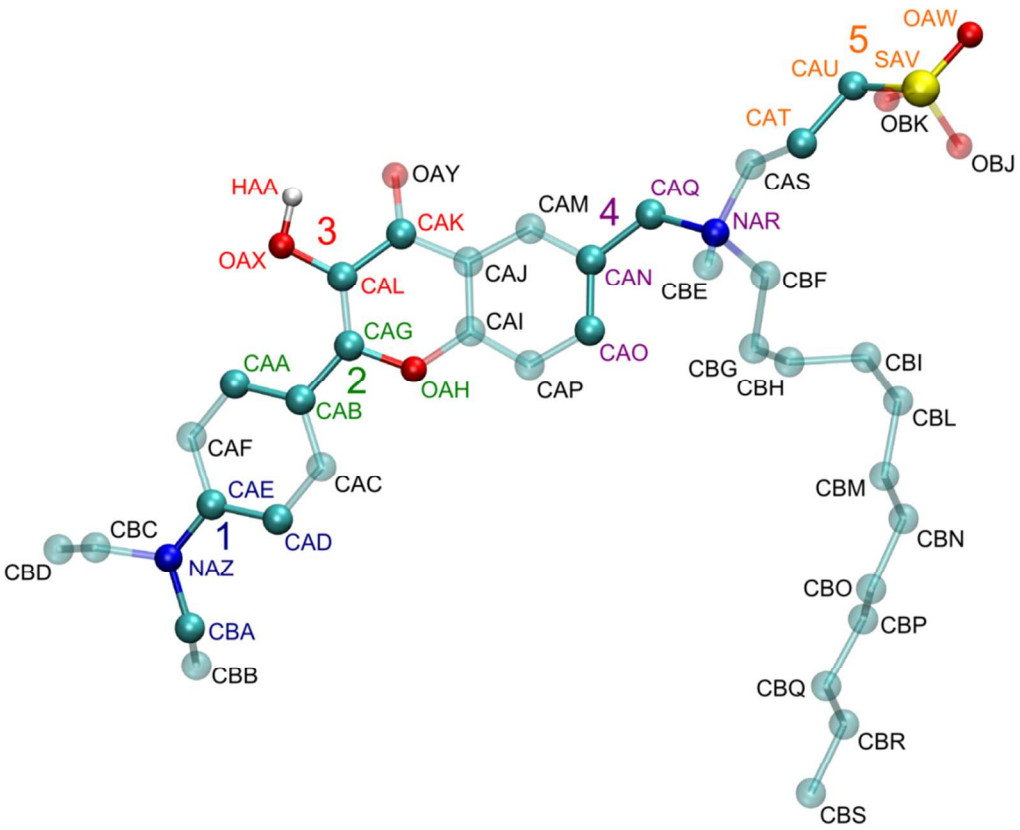

Figure S1. F2N12S dye: atom names and dihedrals (1–5) parameterized by ab initio scans. Color coding: cyan, carbon; red, oxygen; white, hydrogen; blue, nitrogen; yellow, sulfur.

Atom	Atom type	Charge (units of *e*)	Charge group
CBS	LP3	0	1
CBR	LP2	0	2
CBQ	LP2	0	3
CBP	LP2	0	4
CBO	LP2	0	5
CBN	LP2	0	6
CBM	LP2	0	7
CBL	LP2	0	8
CBI	LP2	0	9
CBH	LP2	0.12	10
CBG	LP2	0.07	10
CBF	LP2	-0.09	11
NAR	NL	0.02	11
CAS	CH2	0.07	11
CAT	CH2	0.17	11
CAU	CH2	-0.1	12
SAV	S	1.01	12
OBJ	OM	-0.54	12
OBK	OM	-0.6	12
OAW	OM	-0.58	12
CBE	CH3	0.2	11
CAQ	CH2	0.16	11
CAN	CB	-0.04	13
CAM	CR61	0.11	13
CAO	CR61	0.17	13
CAP	CR61	-0.16	13
CAI	CB	0.4	14
OAH	OS	-0.22	14
CAJ	CB	-0.31	14
CAK	CB	0.44	15
OAY	O	-0.49	15
CAL	CB	0.04	16
OAX	OA	-0.44	16
HAA	HO	0.37	16
CAG	CB	0.09	14
CAB	CB	0.03	17
CAC	CR61	0.02	17

CAD	CR61	-0.16	17
CAA	CR61	0.07	17
CAF	CR61	-0.19	17
CAE	CB	0.42	18
NAZ	N	-0.41	18
CBC	CH2	0.24	18
CBD	CH3	-0.04	19
CBA	CH2	0.23	18
CBB	CH3	-0.04	20

Table S1. Atom types of the modified GROMOS-87 and Berger lipids force fields, atomic charges, and charge groups used to parameterize the F2N12S dye.

2. F2N12S Dihedral Parameterization

Rigid scans of five dihedral potentials (Figure S1) were carried out on molecular fragments by employing the B3LYP functional with the cc-pVDZ basis set. For each dihedral potential, the corresponding molecular fragment is shown in Figure S2. The shape of the dihedral potential was assumed to be

$$V_d(\phi) = \sum_{n=1}^{4} k_n(1 + \cos(n\phi - \phi_n)) \quad \text{(S1)}$$

Parameters k_n and ϕ_n (n=1,…,4) were determined by fitting eq S1 to calculated potentials after subtraction of electrostatic and Lennard-Jones contribution. The resulting values of k_n and ϕ_n are presented in Table S2.

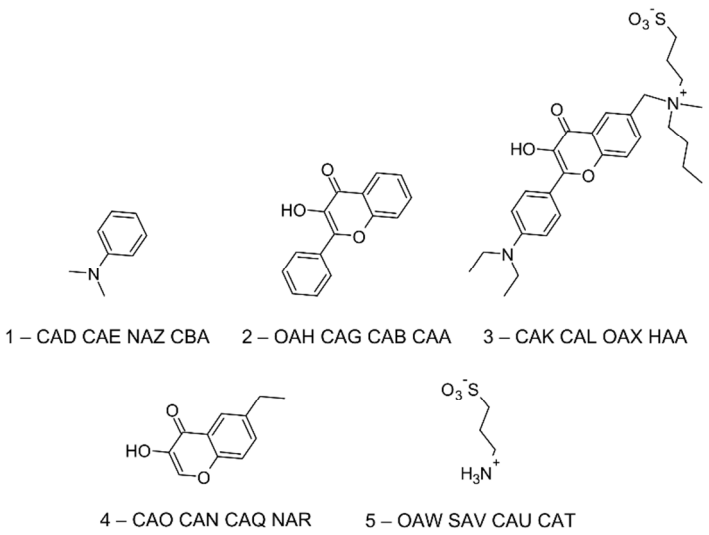

Figure S2. Fragments used for ab initio scans of dihedral potentials.

Dihedral No.	k_1 (kJ/mol)	ϕ_1 (°)	k_2 (kJ/mol)	ϕ_2 (°)	k_3 (kJ/mol)	ϕ_3 (°)	k_4 (kJ/mol)	ϕ_4 (°)
1	0.00	180.00	39.55	182.07	0.36	180.00	2.77	180.00
2	1.55	0.00	23.87	180.10	0.26	0.00	1.02	183.57
3	19.10	182.68	4.02	169.34	6.47	185.04	-1.69	188.64
4	1.56	142.60	13.28	182.93	0.73	63.65	4.03	185.64
5	2.07	45.26	-0.37	60.19	14.53	11.82	-0.34	-78.73

Table S2. Values of dihedral parameters obtained from ab initio scans.

3. Experimental Setup

Figure S3. Experimental setup used for 1P measurements.

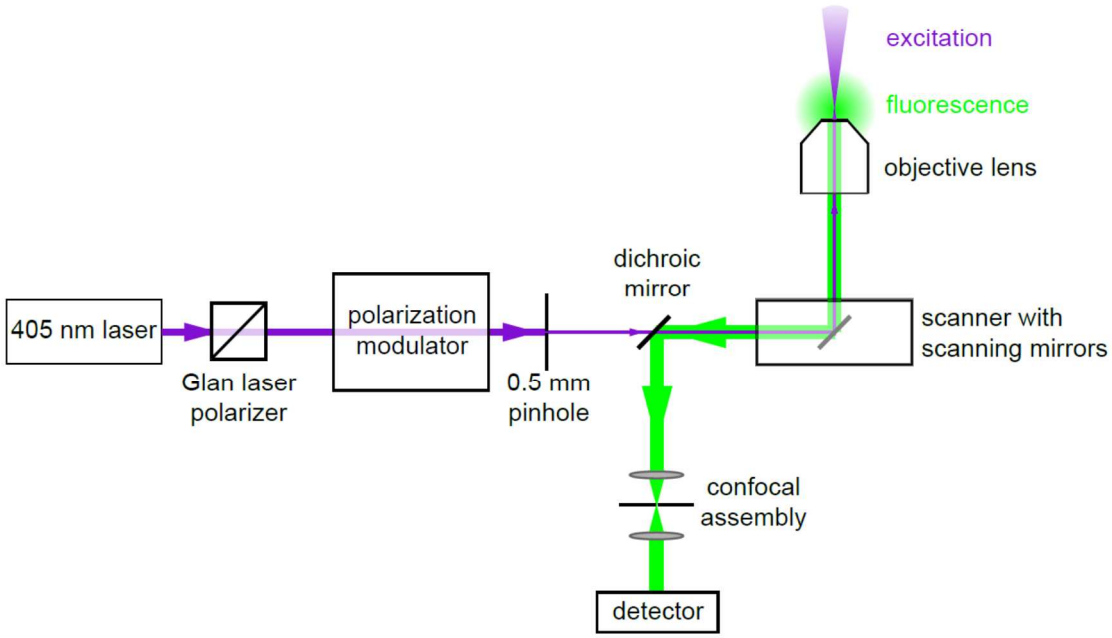

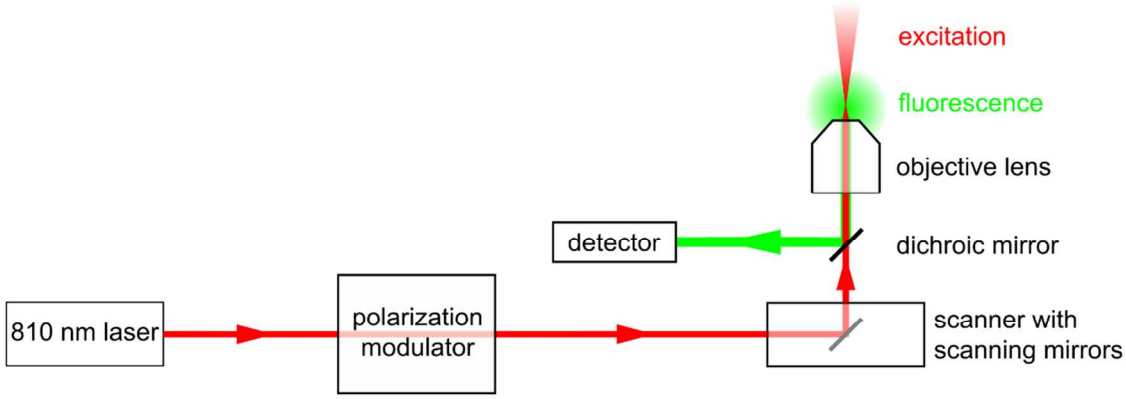

Figure S4. Experimental setup used for 2P measurements.

4. Trajectory Analysis: Interactions of F2N12S in the POPC Bilayer

In addition to the analysis presented in the main text we also analyzed the contacts of the carbonyl oxygen of the dye with water (distance of the water oxygen from the carbonyl oxygen less than or equal to 3.5 Å). We examined the fraction of time the carbonyl oxygen spent in contact with water as a function of the distance of the carbonyl oxygen from the bilayer center. We observed a clear rise in contacts with an increasing distance from the bilayer center (Figure S5A), reflecting the increased hydration of the bilayer in its shallower regions. However, the dependence of the time spent in contact with water on the location of the dye's center of mass was less pronounced (Figure S5B), indicating that the occurrence of more hydrated and less hydrated geometries of the dye correlated more strongly with the tilt of the aromatic rings or the orientation of the carbonyl group than with the depth of the probe as a whole. This is in accord with an analysis of emission spectra in DOPC of a similar dye[1] (F2N8, differing from F2N12S by a shorter alkyl chain and the lack of the SO_3^- anchor), which did not show a significant difference between the depths of the hydrated and non-hydrated geometries in the bilayer. In contrast, a smaller dye F, sharing the same aromatic rings, but adorned with only a dimethylamino group, exhibited a pronounced difference in the depths of the hydrated and non-hydrated geometries.[2]

To gain further information on interactions of the F2N12S dye embedded in the bilayer, we also analyzed the contacts of the OH group of the dye with the sn-1 and sn-2 ester oxygen and sn-1 and sn-2 carbonyl oxygen atoms of the neighboring POPC molecules, with the phosphate groups of the POPC molecules, and with water. Moreover, we investigated the contacts between

water and the heterocycle oxygen of the probe. The results are summarized in Figure S6. We found the OH group of the dye to spend a significant amount of time in contacts with the sn-1 and sn-2 ester oxygen atoms and with the sn-1 carbonyl oxygen while there were virtually no contacts between the heterocycle oxygen of the probe and water. Figure S7 shows results for distinct 100 ns parts of the trajectories.

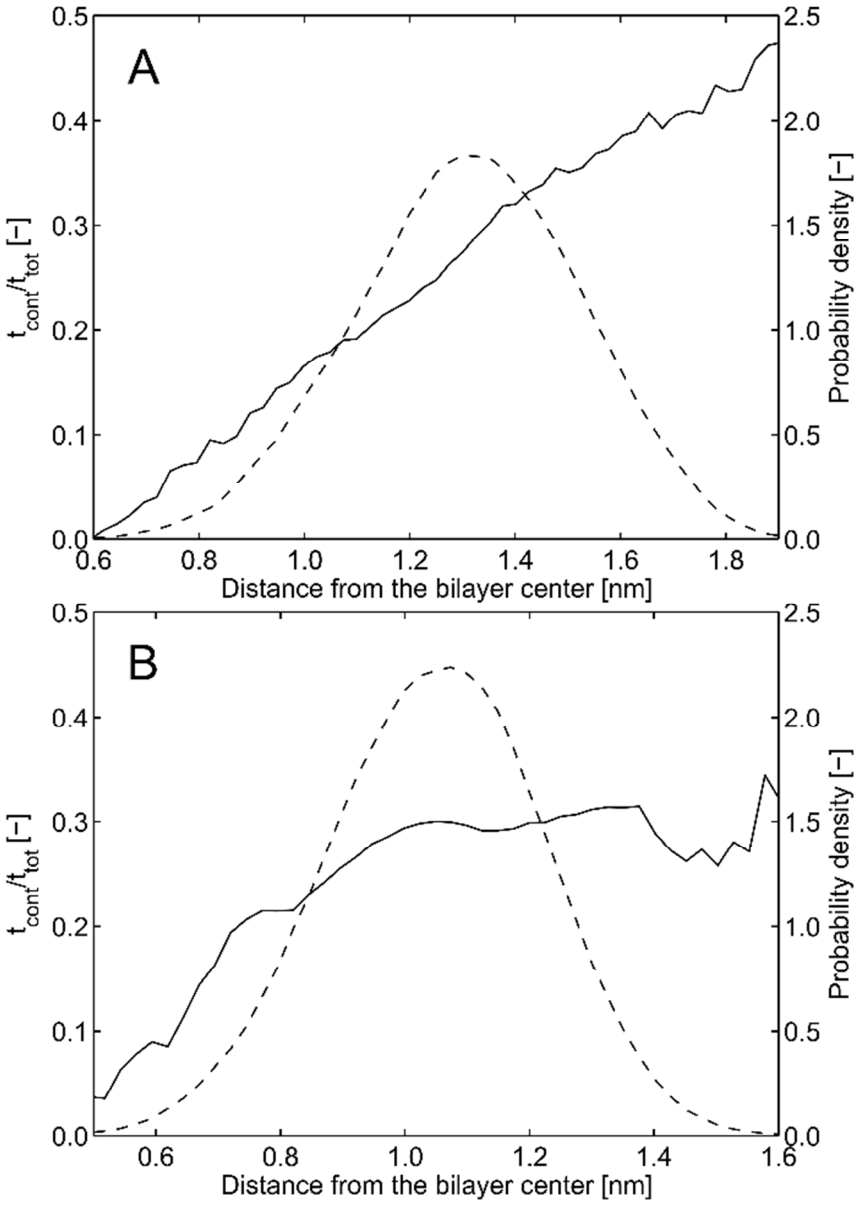

Figure S5. Solid line, fraction of simulation time spent by the carbonyl oxygen of the dye in contact with water depending (A) on the distance of the atom from the bilayer center and (B) on the distance of the dye's center of mass from the bilayer center; dashed line, density profiles of (A) the carbonyl oxygen and (B) the center of mass of the dye.

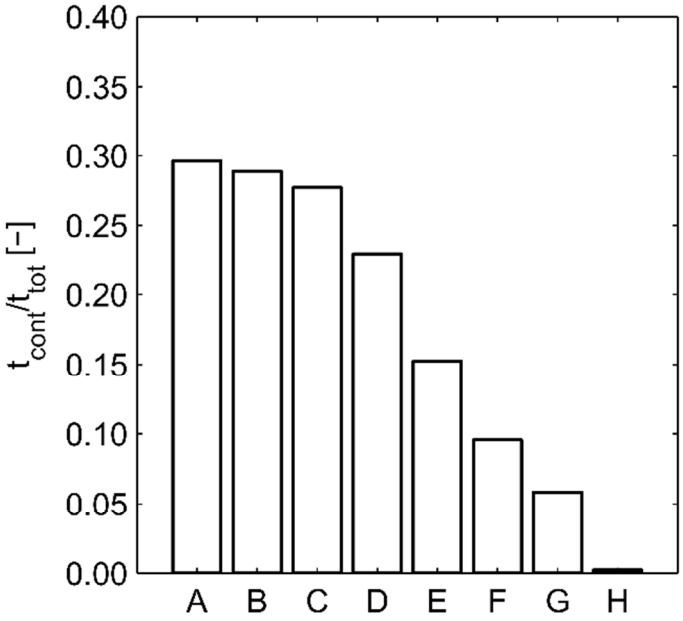

Figure S6. Fraction of total simulation time spent by selected atoms or groups of the dye in contact with water and surrounding POPC molecules. A, OH group and sn-1 ester oxygen; B, OH group and sn-2 ester oxygen; C, carbonyl oxygen and water; D, OH group and sn-1 carbonyl oxygen; E, OH group and water; F, OH group and phosphate; G, OH group and sn-2 carbonyl oxygen; H, heterocycle oxygen and water.

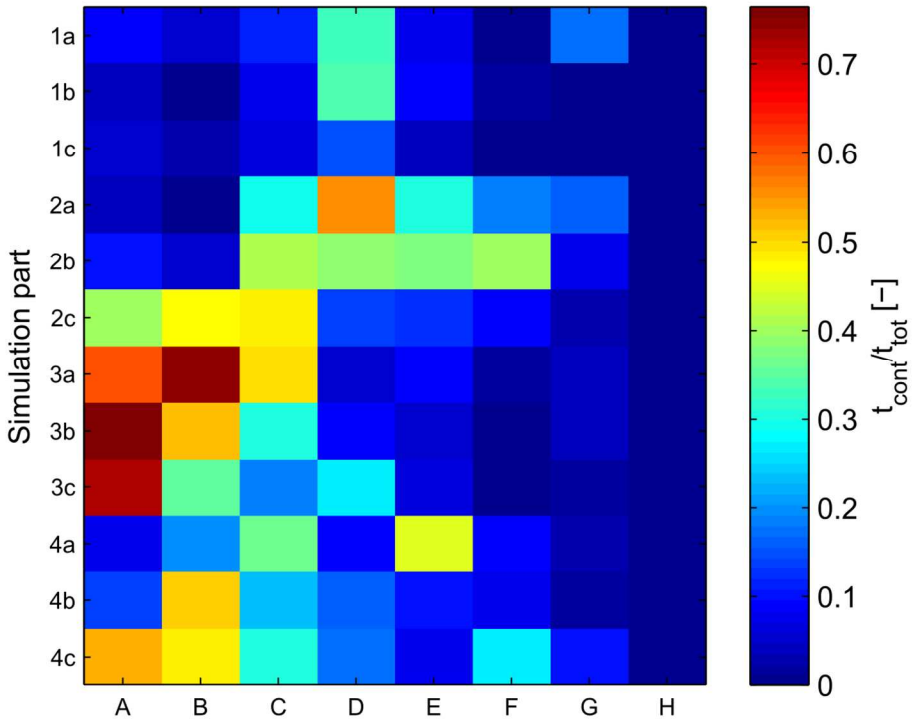

Figure S7. Fraction of simulation time spent by selected atoms or groups of the dye in contact with water and surrounding POPC molecules: separate results for twelve 100 ns parts of the trajectories. A, OH group and sn-1 ester oxygen; B, OH group and sn-2 ester oxygen; C, carbonyl oxygen and water; D, OH group and sn-1 carbonyl oxygen; E, OH group and water; F, OH group and phosphate; G, OH group and sn-2 carbonyl oxygen; H, heterocycle oxygen and water.

5. Trajectory Analysis: Orientational Distributions from Individual Trajectories

Figure S8 shows distributions of the 1PE TDM tilt angle α obtained from four distinct MD trajectories. It demonstrates that even 300 ns sampling times were not sufficient to achieve a perfectly converged situation. While the individual distributions exhibit a large overlap between each other and give a good idea about the character of the orientational distribution, some differences remain in the details of the shapes of the distributions and the exact positions of their peaks.

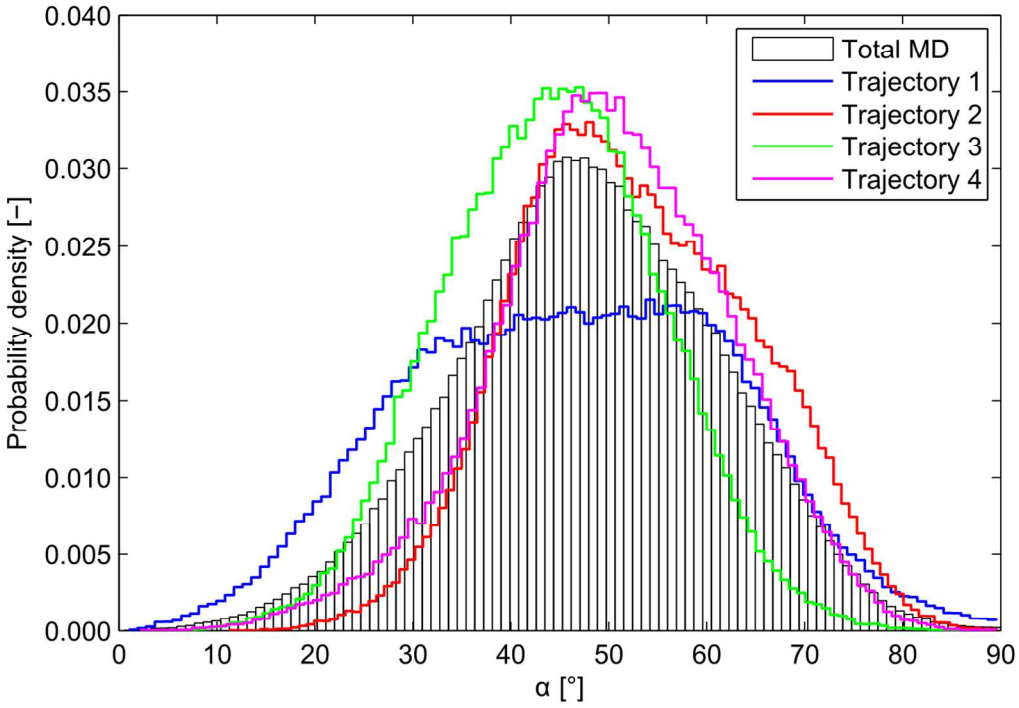

Figure S8. Distributions of the 1PE TDM tilt angle α obtained from individual MD trajectories in comparison to the overall result from MD.

References

(1) Klymchenko, A. S.; Mely, Y.; Demchenko, A. P.; Duportail, G. *Biochim. Biophys. Acta, Biomembr.* **2004**, *1665*, 6.

(2) Klymchenko, A. S.; Duportail, G.; Demchenko, A. P.; Mely, Y. *Biophys. J.* **2004**, *86*, 2929.